Journal of Computer Assisted Tomography
9(4):659–675, July/August

MR Imaging: Clinical Use of the Inversion Recovery Sequence

G. M. Bydder and I. R. Young

Abstract: The properties of the inversion recovery (IR) sequence are considered and its use in clinical practice is illustrated. The effect of changing repetition time, inversion time (TI), and echo time; the method of data encoding; the type of data collection; and the method of image processing are analysed. Normal appearances and clinical examples in the central nervous system and the remainder of the body are used to illustrate the many options available with this sequence. The short TI IR sequence has advantages in magnetic resonance imaging of the body, and medium TI sequences are of value in localisation in the brain and in demonstrating contrast enhancement. Long TI sequences can be used in pediatrics and for separating tumour and oedema. Suppression or partial suppression of fat and fluid signals are two useful options with IR sequences. **Index Terms:** Inversion recovery—Nuclear magnetic resonance, techniques—Nuclear magnetic resonance.

For some time we have been intrigued by the fact that most groups performing magnetic resonance (MR) imaging use spin echo (SE) sequences almost exclusively and make little or no use of the inversion recovery (IR) sequence. Although we make considerable use of the SE sequence and drew attention to its value in imaging of the brain early in the development of clinical MR (1), we also make extensive use of the IR sequence (2–6) and believe that this sequence is in many ways the most interesting of the three sequences in general use. From an imaging point of view both the SE sequence and the partial saturation (PS) sequence can be regarded as limiting cases of the IR sequence, the scope of which includes all the options available with both of these sequences as well as its own unique features. To draw attention to the value of the IR sequence we describe the sequence in nonmathematical terms, discuss the effect of changing different imaging parameters, and illustrate its use in a variety of clinical situations.

From the Department of Diagnostic Radiology, Royal Postgraduate Medical School, Hammersmith Hospital, London (G. M. Bydder), and Picker International, Hirst Research Centre, Wembley, Middlesex (I. R. Young), England. Address correspondence and reprint requests to Dr. G. M. Bydder at Department of Diagnostic Radiology, Royal Postgraduate Medical School, Hammersmith Hospital, Du Cane Road, London W12 OHS, England.

DESCRIPTION OF THE IR SEQUENCE

The dependence of signal intensity seen with the IR sequence on proton density, T1, and T2 has been described in mathematical terms in previous articles in this journal (4,7,8) but our principal interest in this paper is clinical and we will use a qualitative description of the IR sequence.

The prototype Picker imaging machine used in these studies has been described previously (4) and operates at 0.15 T. We can represent the proton magnetisation induced in the patient by the static magnetic field by a vector M. The component of the magnetisation in the transverse plane at any given time is then represented by M_{xy}, and that in the longitudinal direction at the same time by M_z. The effect of a 90° pulse is to rotate M_z into the transverse plane to become M_{xy} (Fig. 1). Following a 90° pulse, M_z increases exponentially from zero with time constant T1 (Fig. 2a) and M_{xy} decays exponentially with time constant T2 (Fig. 2b). At the following 180° pulse M_z is inverted to become $-M_z$ and recovers with a time constant T1 but at *twice* the rate for the earlier longitudinal recovery after the 90° pulse. At the next 90° pulse M_z is rotated to become M_{xy}. M_{xy} then decays exponentially with time constant T2. Using a field echo or free induction decay data collection, signal is collected at a mean echo time (TE) after the 90° pulse and the cycle is repeated (a field echo uses symmetrical gra-

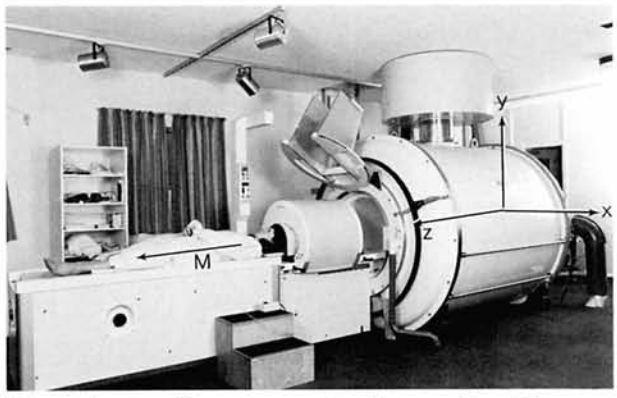

FIG. 1. A magnetic resonance imaging machine. The cryomagnet produces a net magnetisation M in the longitudinal axis of the volunteer; 90° pulses are used to rotate this magnetisation into the transverse plane. The x, y, and z axes are shown.

dient fields to form the echo). We can use a composite diagram following first M_z then M_{xy} after the second 90° pulse to represent the "potential signal intensity" at various stages in the sequence (Fig. 2c) to understand how this may be varied.

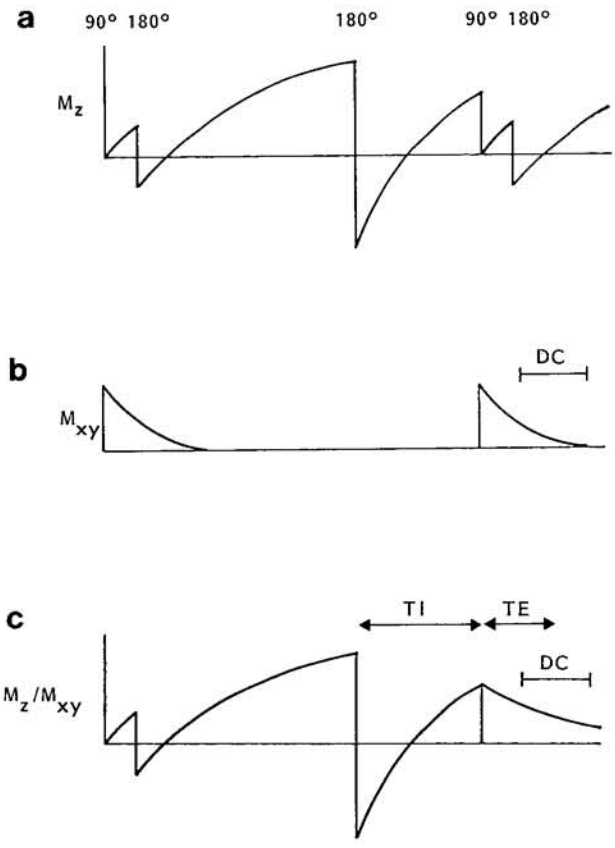

FIG. 3. Changes in M_z **(a)** and M_{xy} **(b)** with time in the inversion recovery sequence (medium inversion time, TI) using a spin echo data collection (DC). **c:** M_z initially and M_{xy} in the last segment. TE, echo time.

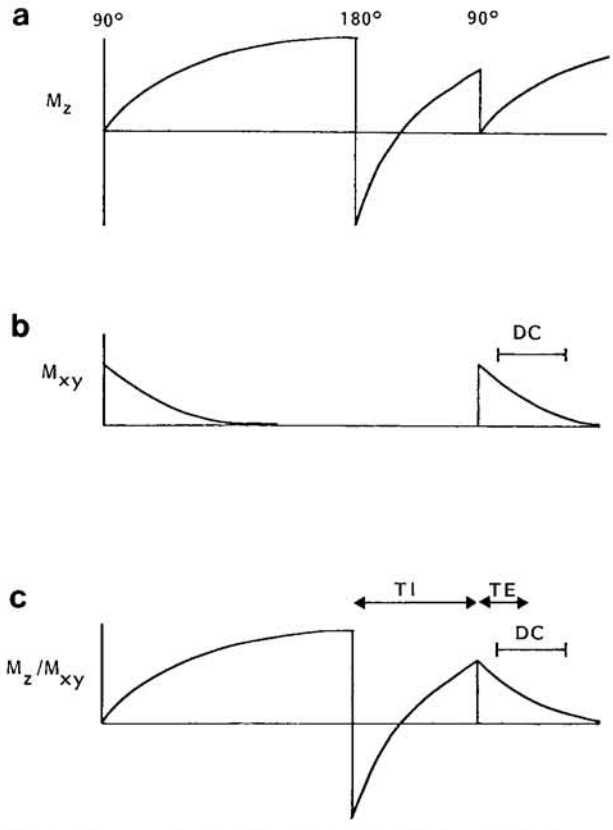

FIG. 2. Changes in M_z **(a)** and M_{xy} **(b)** with time in the inversion recovery sequence (medium inversion time, TI) using a field echo data collection (DC). **c:** M_z in the first two segments and M_{xy} in the last segment. TE, echo time.

In Fig. 3 the corresponding figures are drawn for the situation where an SE pulse is used with an SE data collection in the last stage of the sequence. The figures are similar except that the data collection is delayed compared with the previous case, and the magnetisation is inverted again by the additional 180° pulse (only T2 is considered rather than T2*; additional decay due to field inhomogeneity is reduced as a result of the refocusing 180° pulse). The size of the received signal and ultimately the signal intensity or pixel value in the image is proportional to M_{xy} at the time of the data collection. M_{xy} is also proportional to tissue proton density. The inversion time (TI) and TE as used in the American College of Radiology convention are shown in Figs. 2 and 3. Repetition time (TR) is the duration of each cycle of the sequence, TI is the time between the inverting 180° pulse and the following 90° pulse, and TE is the time from the last 90° pulse to the following echo.

Using Fig. 2c as our model of the IR sequence, we can compare the signal intensities of white matter (a tissue with a relatively short T1), grey matter (a tissue with a longer T1), and cerebrospinal fluid (CSF) (which has a very long T1) in Fig. 4.

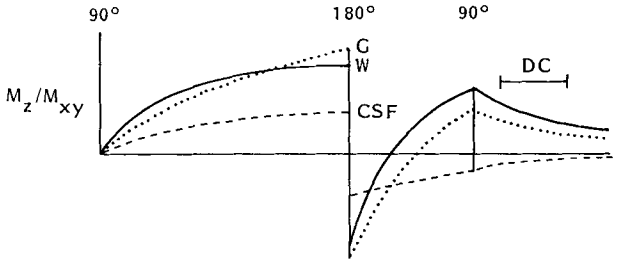

FIG. 4. Changes in M_z/M_{xy} with time in the inversion recovery sequence (medium inversion time) for white matter (W), grey matter (G), and cerebrospinal fluid (CSF) using field echo data collection (DC).

The signal intensity observed is proportional to the height of M_{xy} in Fig. 4, and it can be seen that the shorter T1 of white matter results in a higher signal intensity than for grey matter. The very long T1 of CSF results in a low signal intensity that may be negative as in Fig. 4. Note that the last segment of the decay converges towards zero for both grey and white matter with their positive signal intensities, as well as for CSF with its negative signal intensity. Display of the resultant image after phase corrected processing (see later) gives white for white matter, light grey for grey matter, dark grey for zero signal intensity, and black for CSF. The signal for grey matter is slightly greater than that for white matter at the time of the 180° pulse because of its 10% greater proton density. We next consider the effects of changing TR, TI, TE, the imaging processing technique, and other parameters on the signal intensity at the time of data collection.

Effect of Changes in TR

The general rule is that a time of at least 3T1 should be allowed for recovery of the longitudinal magnetisation between the 90° of the last pulse cycle and the following 180° pulse of the next pulse cycle to allow a high level of recovery of M_z, although, in practice, it is possible to use times less than this. It is important to note: (a) That the rule above applies to all the tissues in a slice and, as many lesions have an increased T1, this sets a lower limit for TR that may be much greater than it would be for normal tissues. (b) It is also important to note that fluids such as CSF, urine, and small bowel contents usually have a very long T1 and do not fully recover with the values of TR in general use. This may be an advantage for some purposes; for example, it may be helpful to have the CSF signal less than brain (see later). (c) Values of T1 at the operating field in this study are listed in Table 1. At higher fields, tissue T1 is increased; for example, at 10 times the static field used here, T1 is approximately doubled for many tissues (9) although fat does not increase this much, and CSF changes relatively little. T2 is essentially unchanged with field.

TABLE 1. *Values of T1, T2, and the ratio of T1/T2 at 0.15 T for various tissues*

Tissue	T1 (ms)	T2 (ms)	T1/T2
Grey matter	453 ± 77	101 ± 13	4.5
White matter	353 ± 60	92 ± 22	3.8
Cardiac muscle	377 ± 60	57 ± 16	6.6
Liver	206 ± 45	43 ± 14	4.8
Spleen	364 ± 69	62 ± 37	5.9
Kidney	368 ± 99	58 ± 24	6.3
Skeletal muscle	330 ± 59	47 ± 13	7.0
Fat	173 ± 49	84 ± 36	2.1

From ref. 9.

Reducing TR produces a reduction in signal intensity for tissues with a long T1, although there is little effect on tissues with a short T1 where TR is still greater than 3T1. Reducing TR is therefore used to reduce the relative signal intensity of tissues, such as the spleen, which have a long T1, or of fluids, such as CSF, which have a very long T1 (see later). There is little advantage in increasing TR beyond 3T1.

Effect of Changes in TI

It is useful to consider three variants of the IR sequence according to their values of TI: (a) short TI (TI approximately 0–250 ms); (b) medium TI (TI approximately 250–700 ms); (c) long TI (TI approximately 700 ms and longer). These TI categories are applicable at 0.15 T. The approximate factors by which to multiply TI and TR to achieve the same effects at higher fields by compensating for the increase in tissue T1 are listed in Table 2 (derived from ref. 9).

Short TI

The values of T1 included here are approximately 0–250 ms. In the limit where TI equals zero (or, from a practical point of view approximately 1 ms) the 90 and 180° pulses add to give a 270° pulse that

TABLE 2. *Ratio of T1 at different fields to that at 0.15 T for various tissues*

Tissue	Field strength (T)				
	0.15	0.3	0.5	1	1.5
Grey matter	1	1.24	1.45	1.79	2.03
White matter	1	1.27	1.52	1.93	2.23
Cardiac muscle	1	1.28	1.55	1.99	2.30
Liver	1	1.30	1.58	2.05	2.39
Spleen	1	1.24	1.49	1.88	2.15
Kidney	1	1.19	1.35	1.60	1.77
Skeletal muscle	1	1.34	1.66	2.22	2.63
Fat	1	1.13	1.24	1.39	1.50

From ref. 9.

is equivalent to a −90° pulse. Using magnitude reconstruction (see later), this is equivalent to a 90° pulse and the sequence in Fig. 2c becomes 90°-data collection, or the PS sequence. Thus, the PS sequence can be regarded as a limiting case of the IR sequence with TI = 0. The same reasoning applies when an SE data collection is used (Fig. 3c) and the IR sequence (with TI = 0) becomes equivalent to an SE sequence. This is the basis for regarding both the SE and the PS sequences as limiting cases of the IR sequence. Using magnitude reconstruction with TI in the range of 0 to approximately 250 ms, an IR image of the brain appears like an SE one although with greater grey-white matter contrast. The magnetisation curves can be represented as shown in Fig. 5. Note that following the final 90° pulse the T1 contrast and the T2 contrast are *additive*, i.e., increasing the T1 of a tissue increases the relative signal intensity of the tissue and so does increasing its T2. (This is *not* the case in Fig. 2c or Fig. 3c, which illustrate medium values of TI.) The short TI IR (STIR) sequence is sensitive to changes in T1 and T2 and can be used as a screening sequence in the brain in a similar way to SE sequences with long TE and long TR such as $SE_{1,500/80}$. To reduce the signal intensity of CSF to less than that of white matter, TR can be shortened, as suggested in the previous section, to 1,000 ms with a sequence such as $IR_{1,000/100/44}$.

Since many pathological lesions produce an increase in both T1 and T2, the addition of these two types of contrast with the STIR sequence produces high net tissue contrast. This type of sequence also enables some T1 dependent decay to be substituted for the T2 dependent decay in the equivalent SE sequence. This is of particular value where the T1 and T2 decays of the tissues differ and explains why the grey-white matter contrast of this sequence is greater than the equivalent SE sequence. In the body there is another reason for making this substitution when an SE data collection is used, as it allows a reduced value of TE for equivalent soft tissue contrast thus reducing the vulnerability of the sequence to motion.

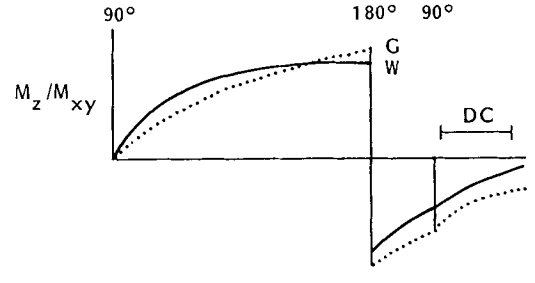

FIG. 5. Changes in M_z/M_{xy} time for a short inversion time inversion recovery sequence. The magnitude of the signal from grey matter (G) is greater than that for white matter (W) using field echo data collection (DC).

It is also possible to choose particular values of TI so that the signal intensity of a particular tissue is zero at the time of the 90° pulse (Fig. 6). (This occurs at a value of TI typically between 0.56 and 0.69 T1 for TR > 3T1.) Values of approximately 100 ms are suitable to eliminate the fat signal, and 255 ms is adequate for white matter. In this situation the tissue signal is said to be "suppressed." Suppression or partial suppression of the fat signal is of particular value in the orbit, breast, and abdomen. In the abdomen respiratory artefact frequently arises from subcutaneous fat and reduction of the fat signal minimises this. In addition, SE sequences with long TE and TR produce a relatively high signal intensity from soft tissue lesions that have an increased T2, but since fat also has a long T2 these lesions may be indistinguishable from fat. Suppression or partial suppression of the fat signal avoids this problem. Other uses of these sequences include suppression of the high signal from fat adjacent to a surface coil and the suppression of the signal from liver to highlight lesions.

Medium TI

The working rule to obtain an image with good contrast between two tissues of different T1 values is to choose a value of TI intermediate between the two tissues of interest (neglecting the effects of proton density and T2), so that satisfactory contrast between white matter (T1 = 350 ms) and grey matter (T1 = 450 ms) is achieved with a TI of approximately 400 ms. Note that the signal intensity is not maximal at this point so the image appears noisier than that obtained with, for example, TI = 500 ms where the signal is higher (although the grey-white matter contrast is less). In theory maximum contrast is obtained when TI is approximately 0.65 times the average of the T1 for the two tissues, but the signal levels in this case are close to zero, and

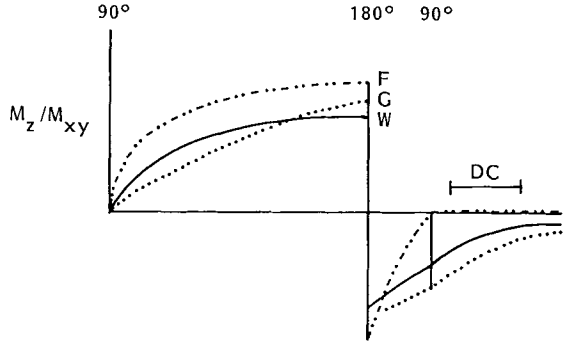

FIG. 6. Changes in M_z/M_{xy} with time for fat (F), white matter (W), and grey matter (G) using a fat suppressed short inversion time inversion recovery sequence. The signal from G is greater than that for W and F gives no signal using field echo data collection (DC).

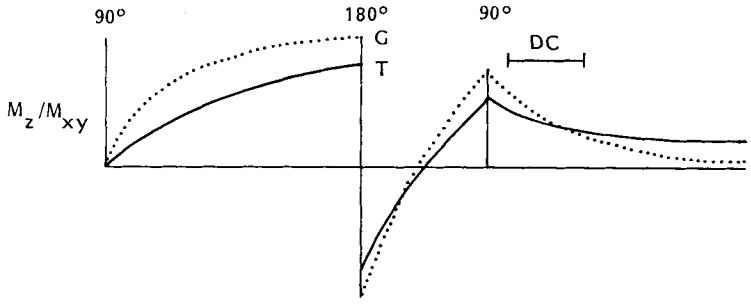

FIG. 7. Changes in M_z/M_{xy} with time for grey matter (G) and a tumour (T) using a medium inversion time inversion recovery sequence. There is a relative reduction in the signal from T during the first two segments of the sequence (T1 dependent section) but a relative increase in the last section (T2 dependent section) using field echo data collection (DC).

maximise the appearance of the noise in the image. Note that the TI for optimum contrast between grey and white matter will not be optimal for that between grey matter and a tumour that has an increased T1 (Fig. 7).

There are two additional modifying factors. The increased mobile proton density of grey matter relative to white matter results in slightly less tissue contrast. More important is the fact that the T2 dependent period following the 90° pulse and prior to data collection may produce a *reduction* in tissue contrast. This is particularly so for lesions that follow the common pattern in which T1 and T2 are both increased. The T2 dependent decay, in the last component of the sequence, reduces the T1 contrast developed earlier in the sequence.

The method of image reconstruction and the type of data collection affect TE. Echo time is generally shorter with projection-reconstruction than with two-dimensional Fourier transformation (2DFT) since a single vector encoding gradient is used, without the need for a previous phase encoding period as with 2DFT. A field echo data collection can be completed earlier than an SE collection with the same band width, although the former is more vulnerable to B_0 field inhomogeneities.

With the brain (T2 approximately 100 ms), the T2 dependence of the IR sequence is not such a big problem as it is in the body where values of T2 are typically half those in the brain (45–60 ms) making the same IR sequence much more T2 dependent than when it is used in the brain. The use of short values of TE to control this problem becomes important. The alternative is to use short values of TI so that the T1 and T2 contrast after the 90° pulse is additive as outlined in the previous section.

Long TI

For reasons outlined above these sequences may be useful in separating tumour from oedema (where both have increased values of T1). Sequences designed for this purpose require an increase in the value of TR. They are also useful in pediatrics where the T1 of normal brain may be increased 3–400% when compared with adults (5). Another use is suppression of long T1 fluids such as CSF, urine, and bowel contents where values of T1 of 800–1200 ms can be used. It is also possible to use a "double" IR (DIR) with the first TI (e.g., TI1 = 1,200 ms) used to suppress a fluid and the second TI (TI2 = 100 ms) used to suppress fat (e.g., $DIR_{3,000/1,200/100/44}$) (Fig. 8) although this type of sequence is slow and may show some reduction in lesion contrast. The value of TI required to suppress small bowel contents is less than that for purer fluids such as CSF.

Effect of Changes in TE

Increasing TE increases the T2 dependence of the IR sequence. This is useful for short TI sequences, generally not useful for medium TI sequences, and of limited value for long TI sequences.

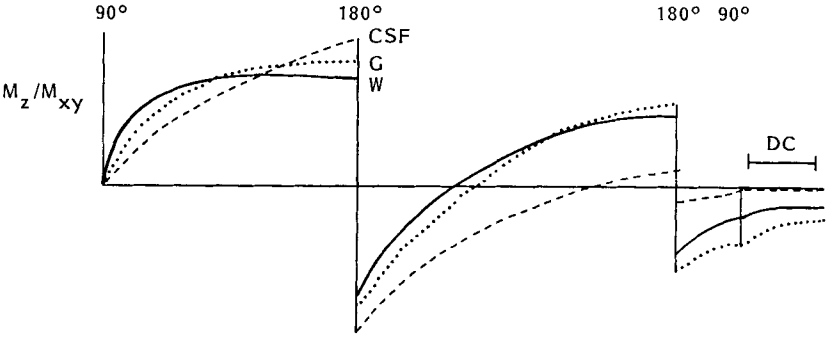

FIG. 8. Changes in M_z/M_{xy} with time for CSF, white matter (W), and grey matter (G) for the double inversion recovery sequence. The signal from G is greater than that for W and cerebrospinal fluid (CSF) gives no signal using field echo data collection (DC).

Short TI

The rule for maximum contrast for SE sequences is to use TE halfway between the T2 values of the two tissues of interest (neglecting proton density and T1 effects). It is most useful to increase TE when imaging tissues with a long T2 such as spleen or kidney (and of course brain). The rule for STIR sequences is to use TE rather less than this value because of the additional T1 dependent contrast. Additional echoes can be usefully added to this type of sequence.

Medium TI

In general TE should be reduced to a minimum. Projection-reconstruction with a field echo data collection may be used for this purpose.

Long TI

Echo time can be increased with this type of sequence to increase the relative T2 dependence although the contrast may be ambiguous unless TI is quite long (as for the DIR sequence).

Effects of Methods of Processing

There are two types of image reconstruction available—*phase corrected* where positive values of signal intensity are shown positive and negative values appear negative, and *magnitude* reconstruction where the magnitude of the signal is used irrespective of its sign. For STIR sequences using phase corrected processing white matter is white and grey matter is grey but the reverse is so with magnitude processing (10). For medium TI sequences the CSF appears dark with phase corrected processing but may show a "rebound" with a lighter central area with magnitude processing. The signal intensities follow directly from considering Figs. 4 and 5.

Effects of Multislice or Single Slice Imaging

The 90° pulse in the IR sequence is always slice selected, although for single slice scans the 180° pulse(s) need not be. However, when the IR sequence is used to obtain an interleaved set of slices, 180° pulse(s) must be slice selected. When the 180° pulse is slice selected, it is possible for flowing blood to experience only part of the IR sequence depending on where it is at the times of the inversion pulses. For example, blood flowing into a slice may only experience a 90° pulse and behave as though it is being imaged with a PS sequence producing a high signal intensity rather than the usual low signal intensity.

CLINICAL ILLUSTRATIONS OF THE USE OF THE IR SEQUENCE

Many of the applications of the IR sequence follow directly from considerations in the previous section. Typical sequences and their applications in the central nervous system (CNS) and in the body are listed in Table 3 and some of these are illustrated below.

Applications in the CNS

The STIR sequences can be used for disease detection (Fig. 9). Both TR and TI can be adjusted so that one version of the sequence generates images with the signal intensity of CSF slightly less than that of white matter in order that periventricular lesions can be recognised without confusion from partial volume effects, and the other version generates images with the CSF signal greater than that of brain (Fig. 10).

Separation of tumour from oedema may also be accomplished (Fig. 11), and additional lesions may also be seen in vascular disease (Fig. 12). Medium TI IR scans provide localisation of disease, assessment of mass effects, and developmental information in older infants. Contrast enhancement is usually maximal with this sequence (11) (Fig. 13). The sequence also provides a better technique for computing T1 maps than that using two SE sequences.

"Short T1 short T2" tumours including some meningiomas and some acoustic neuromas are well demonstrated with medium TI IR sequences (Fig. 14) as are subacute hemorrhage and usually multiple sclerosis (MS) lesions in the brain stem. Long TI IR sequences may help in distinguishing tumour from oedema as well as in pediatric applications (Fig. 15). The DIR sequence can be used to suppress CSF (Fig. 16) as well as to suppress bile ducts and urine. Some cord lesions are better defined with the IR sequence (Fig. 17).

Applications in the Body

Mediastinal and chest wall lesions can be well displayed with the STIR sequences. This avoids confusion of fat with long TE sequences and the confusion of lung with tumour using medium TI IR sequences although fat can also be a valuable marker of tissue planes.

The STIR sequences are of value in imaging the abdomen and pelvis. In Fig. 18 a contrast enhanced CT scan is compared with an $IR_{1,500/100/44}$ sequence. The extent of the tumour in the left lobe of the liver is better shown on the IR scan. Dilated bile ducts are also highlighted. Using a DIR sequence in a patient with metastases to the liver, an additional metastasis is seen in the right adrenal gland (Fig.

TABLE 3. *Typical inversion recovery sequences (at 0.15 T)*

Purpose	TR (ms)	TI (ms)	TE (ms)	Field/ spin echo (F/S)	Reconstruction (PR/2DFT)	Processing Phase corrected (PC) or magnitude (M)	Resolution	Comment
Brain and spinal cord								
Disease detection [cerebrospinal fluid (CSF) signal less than white matter]	1,500	80	44	S	2DFT	M	256 × 256	
	1,000	100	44	S	2DFT	M	256 × 256	
Disease detection (CSF signal greater than white matter)	1,500	100	44	S	2DFT	M	256 × 256	
	2,000	100	80	S	2DFT	M	256 × 256	
	1,200	200	8	F	PR	M	115 × 115	Older sequence
Adult anatomy and localisation	1,500	500	44	S	2DFT	PC	256 × 256	
	1,400	400	5	F	PR	PC	115 × 115	Older sequence
Pediatric development and localisation	3,000	1,000	44	S	2DFT	PC	256 × 256	Premature infant
	2,400	800	44	S	2DFT	PC	256 × 256	0–3 months
	1,800	600	44	S	2DFT	PC	256 × 256	3 months–2 years
Contrast enhancement	1,500	500	44	S	2DFT	PC	256 × 256	
	1,400	400	13	F	PR	PC	115 × 115	Less T2 dependent than sequence above
CSF suppression (DIR)	3,000	1,200 100	44	S	2DFT	M	256 × 256	
Orbital fat suppression	1,500	100	44	S	2DFT	M	256 × 256	
Body								
Mediastinal mass	1,500	100	44	S	2DFT		256 × 256	Cardiac gated and ROPE
Myocardium	Double beat	600	13	F	2DFT	M	128 × 192	Cardiac gated and ROPE
Liver and pancreas	1,500	100	30	S	2DFT	M	256 × 256	With ROPE
	1,500	100	44	S	2DFT	M	256 × 256	With ROPE
	1,000	100	44	S	2DFT	M	256 × 256	With ROPE
	1,400	400	13	F	2DFT	PC	128 × 192	With ROPE
Contrast enhancement	1,400	400	13	F	2DFT	PC	128 × 192	(positive enhancement)
Spleen and kidney	1,500	100	60	S	2DFT	M		
	1,500	100	80	S	2DFT	M		
Pelvis DIR	3,000	1,000 100	44	S	2DFT	M	256 × 256	
Bone	1,500	500	44	S	2DFT	PC	256 × 256	
	1,500	100	44	S	2DFT	M	256 × 256	

Abbreviations: CSF, cerebrospinal fluid; DIR, double inversion recovery; PR, projection reconstruction; ROPE, respiratory ordered phase encoding; TE, echo time; TI, inversion time; TR, repetition time; 2DFT, two-dimensional Fourier transformation.

19). Lobar atrophy is seen associated with a hemangioma in Fig. 20.

In Fig. 21 contrast enhanced CT, $IR_{1,500/100/44}$, $SE_{544/44}$, and $SE_{1,500/80}$ scans are compared. The abscess, thickened abnormal abdominal wall, fluid tracking posteriorly, and paraaortic lymph node are best displayed with the IR sequence.

The margin between tumour and normal bone marrow is better shown with the IR scan than with the SE scan in Fig. 22. Separation of tumour and fatty marrow (both of which have a long T2) by use of STIR sequences (exploiting the short T1 of fat) may be useful although care is necessary to distinguish red marrow from tumour.

DISCUSSION

With the range of options and apparent advantages outlined above, why is the IR sequence used so little in clinical practice? There is probably no straightforward answer to this question but a number of possible explanations are listed below.

1. *The IR sequence is generally thought of only as the medium TI variant.* Very little attention has been paid to the short TI and long TI variants of the IR sequence although they were described early in the development of MR (2) and offer many useful options at both high and low fields.

2. *The significance of the T2 dependence of the medium TI IR sequence has not been fully appreciated.* Since many lesions produce an increase in both T1 and T2, the T2 dependence of the IR sequence produces a net reduction in the T1 dependent contrast. To obtain useful disease detection with a medium TI IR sequence, TE should be kept as short as possible. This was done in earlier studies

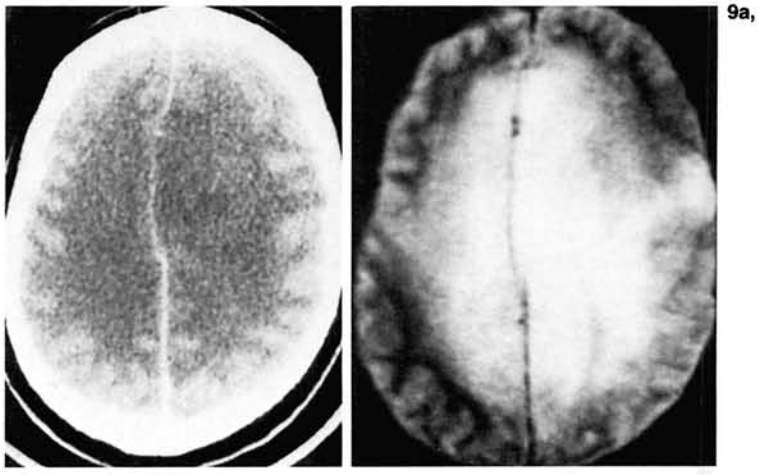

FIG. 9. Frontoparietal astrocytoma grade II: contrast enhanced CT **(a)** and inversion recovery $(IR)_{1,000/100/44}$ **(b)** scans. The tumour is seen to be bilateral in (b). (A central artefact is noted on this and some subsequent scans.)

with projection-reconstruction and field echo data collection (2,3). The more recent use of 2DFT and SE data collection has resulted in longer values of TE being used with more T2 dependence. In addition, since body tissue T2 values are half those of the brain (excepting fat), the relative T2 dependence of the IR sequences is increased in body examinations producing even further net loss of lesion contrast and decreasing the apparent usefulness of the medium TI IR sequence.

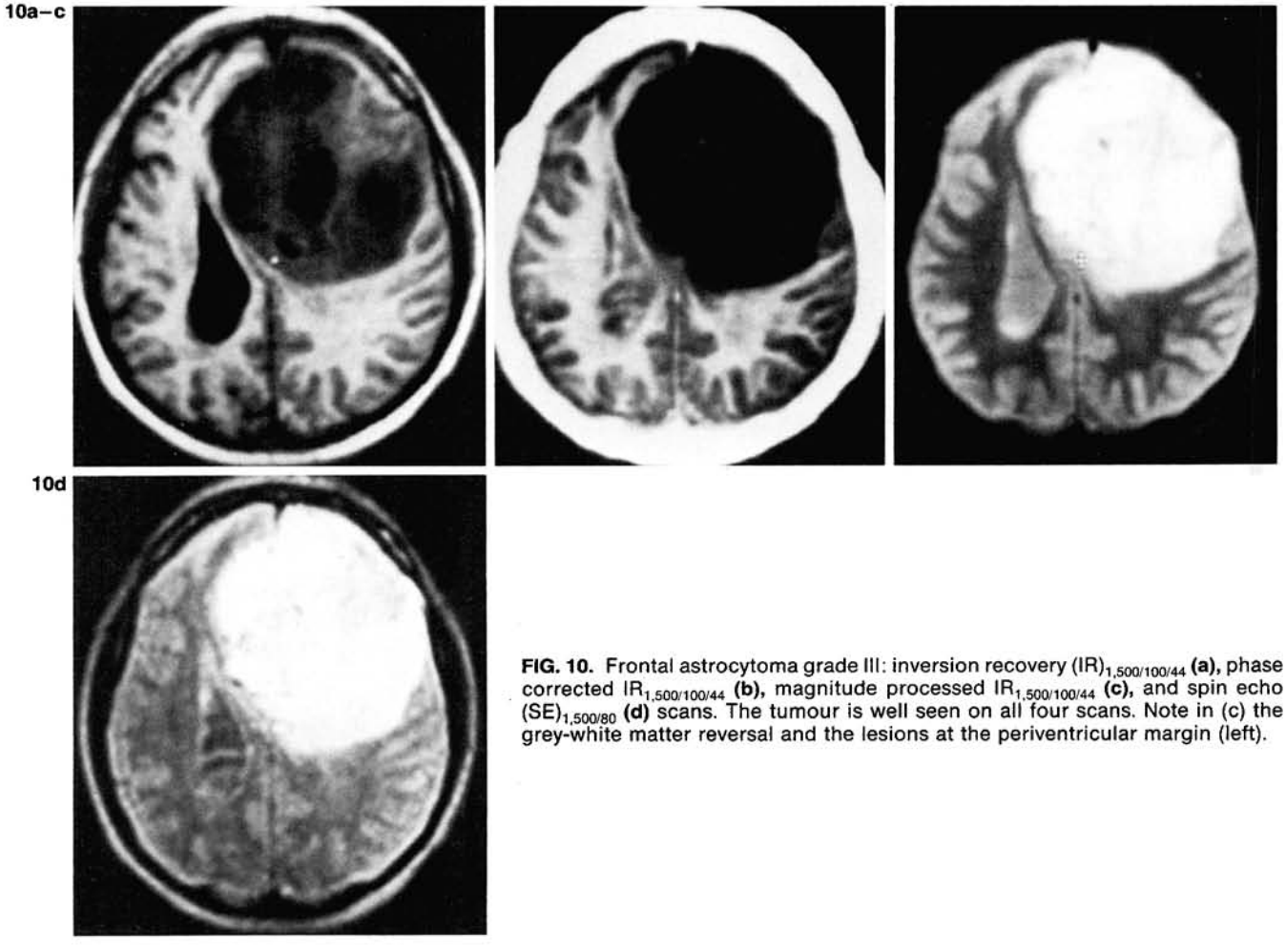

FIG. 10. Frontal astrocytoma grade III: inversion recovery $(IR)_{1,500/100/44}$ **(a),** phase corrected $IR_{1,500/100/44}$ **(b),** magnitude processed $IR_{1,500/100/44}$ **(c),** and spin echo $(SE)_{1,500/80}$ **(d)** scans. The tumour is well seen on all four scans. Note in (c) the grey-white matter reversal and the lesions at the periventricular margin (left).

11a–c

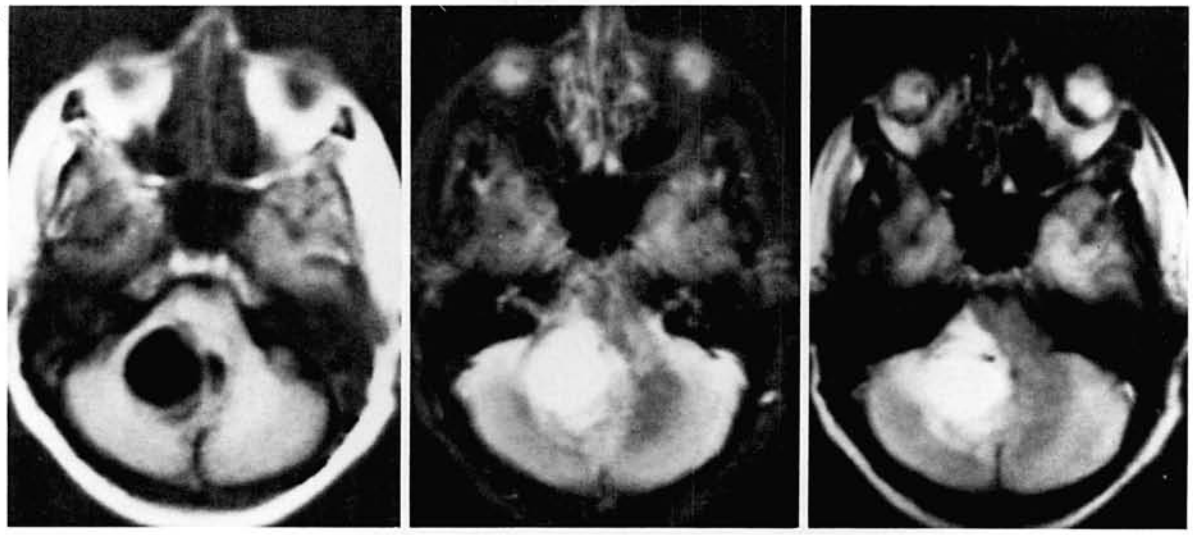

FIG. 11. Cerebellar astrocytoma grade II: inversion recovery $(IR)_{1,500/500/44}$ **(a),** $IR_{2,000/100/44}$ **(b),** and spin echo $(SE)_{1,500/80}$ **(c)** scans. Separation of tumour from oedema is better with the IR scans. The cerebrospinal fluid signal is greater than brain in (b).

3. *The IR sequence has been thought of as "noisy."* Medium TI sequences of the brain provide a quick visual assessment of three machine parameters: tissue contrast, spatial resolution, and noise level. Grey-white matter contrast provides an assessment of tissue contrast; resolution can be assessed by looking at fine anatomical detail (e.g., the cerebellar vermis); and noise level can be assessed by looking at the background, as well as tissues or structures with a very low proton density or those with a moderately long T1, since with a phase corrected IR scan random noise appears in the middle of the grey scale. If the sequence is modified to improve any one of these factors, one or both of the others will suffer to some degree and this is relatively easy to assess on an image. The same type of analysis is not so straightforward on an SE image, as assessment of tissue contrast is not so easy since grey-white matter contrast is less (and a function of proton density in any case), and noise, although present in the image, is at one end of the grey scale and can be "windowed" out. Hence, in comparison with high resolution low noise SE sequences with short values of TE and TR, medium TI sequences appear noisy. However, it is being increasingly accepted that the most useful SE sequences in clinical practice are those with a long TE (1,12), and this type of sequence is more "noisy" than the short TE short TR SE sequence so that the noise levels for comparable disease sensitivity of SE sequences is similar to that of the equivalent IR sequence. Thus, $IR_{1,500/80/44}$ and $SE_{1,500/80}$ sequences show similar disease sensitivity and similar noise levels.

Both with the SE (long TE and long TR) and IR sequences improvements in machine signal/noise

12a,l

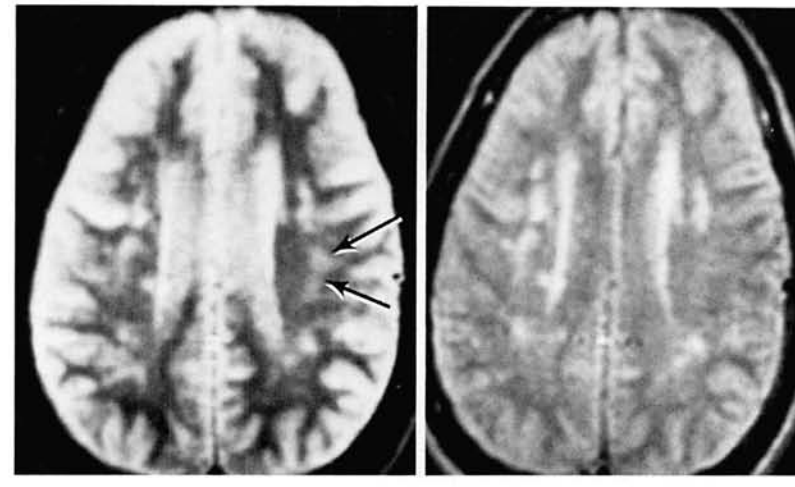

FIG. 12. Cerebrovascular disease: inversion recovery $(IR)_{1,500/100/44}$ **(a)** and spin echo $(SE)_{1,500/80}$ **(b)** scans. Note that some lesions in the left centrum semiovale are better seen in (a) (arrows).

13a–c

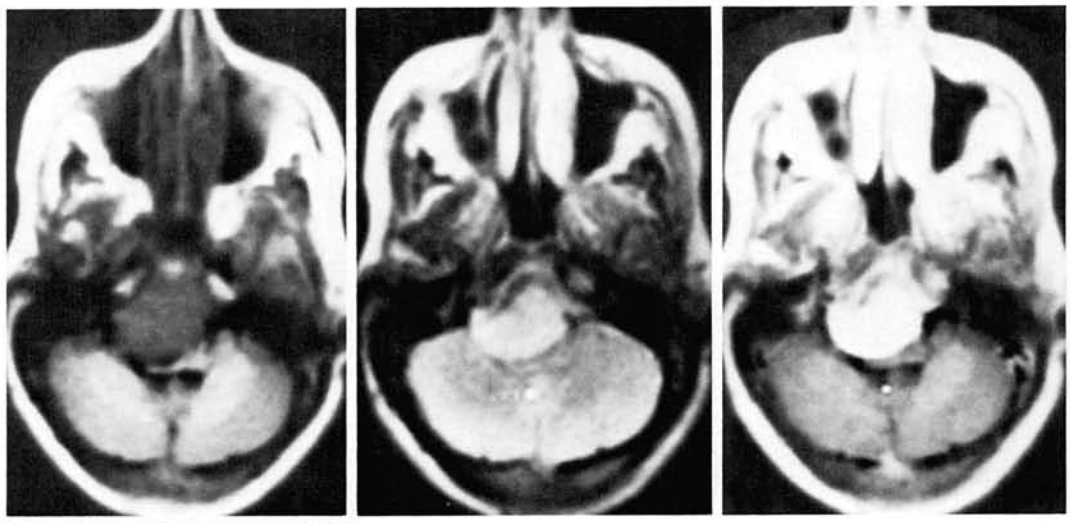

13d

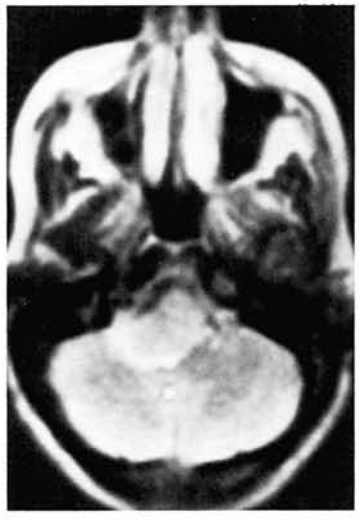

FIG. 13. Clivus meningioma: inversion recovery $(IR)_{1,500/500/44}$ **(a)** and spin echo $(SE)_{1,500/80}$ **(b)** scans before intravenous Gd-DTPA compared with $IR_{1,500/500/44}$ **(c)** and $SE_{1,500/80}$ **(d)** scans after enhancement. Marked enhancement is seen in (c) but little change is evident in (d).

14a,b

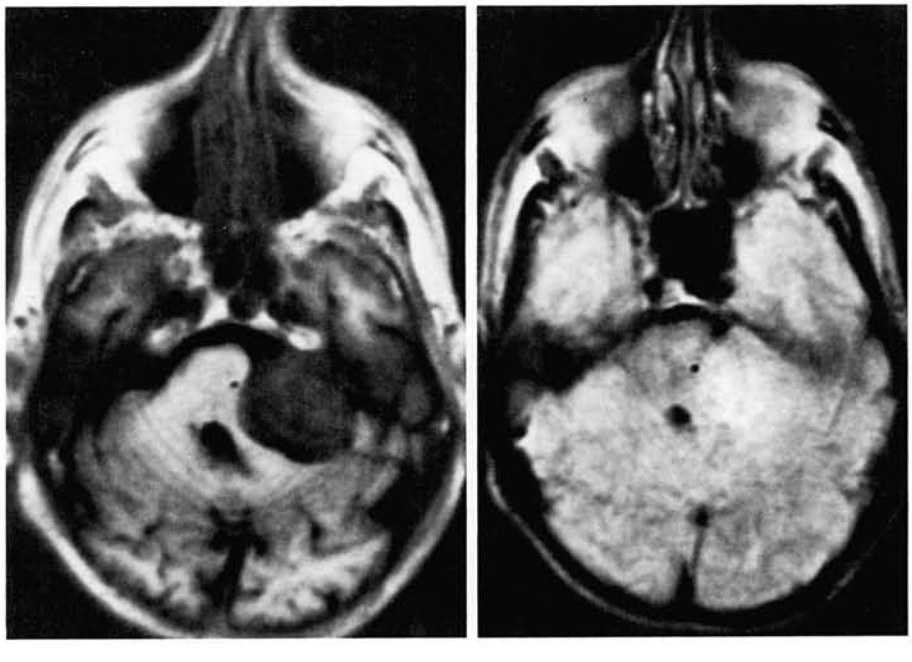

FIG. 14. Acoustic neuroma: inversion recovery $(IR)_{1,500/500/44}$ **(a)** and spin echo $(SE)_{1,500/80}$ **(b)** scans. The tumour is better defined in (a).

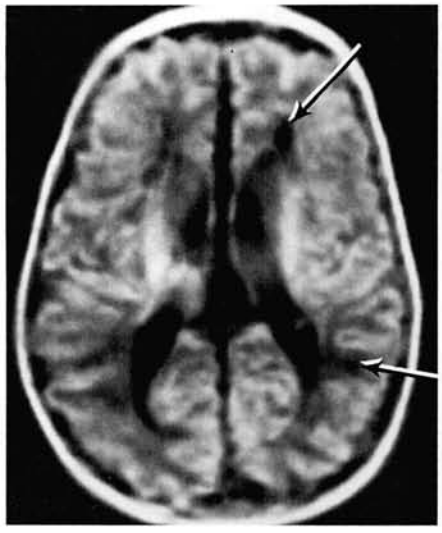

FIG. 15. Cystic leucomalacia in a 3-week-old neonate: inversion recovery $(IR)_{3,000/1,000/44}$ scan. The cysts are well shown (arrows).

ratio result in improved image quality. Methods of improving signal/noise ratio with surface and closely coupled coils have recently been or are soon to be published in this journal (13–15).

4. *The IR sequence is said to be "slow."* This is regarded as less of a problem since the clinical limitations of SE sequences with short TE and short TR have been more widely recognized and SE sequences with long TE and long TR have come into more general use. The use of interleaved slices also provides time to do additional slices during the relatively long TR of the IR sequence. A genuine disadvantage of IR is the fact that with medium and long TI IR sequences it is more difficult to construct an interleaved multislice set because of the relatively isolated 180° inverting pulses, than it is for a comparable SE multislice set. This limitation does not apply to short TI IR sequences to the same extent. The DIR sequence is slow but its use is generally confined to specialised applications.

5. *"It is not possible to obtain useful additional echoes with the IR sequence."* Additional echoes can be obtained with all three groups of IR sequences. They increase T2 dependent contrast with the STIR sequence in a straightforward manner analogous to multiple echo SE sequences, but, with medium TI IR sequences, T1 and T2 contrast are moving in opposite directions and confusing images may result. Additional echoes with these sequences are generally of little value but may be of use in providing a range of T1 and T2 dependent weightings that can be useful in separating tumour from oedema or in its calculation of tissue parameters. With long TI IR sequences (e.g., the DIR sequence) additional SE can be used effectively.

6. *Practical problems.* There are some more specific problems with particular variants of the IR sequence that are worth listing: (a) Partial volume effects with medium TI IR sequences between grey and white matter of the brain may simulate brain lesions. This can be reduced or avoided by using short TI variants. (b) The phase corrected version of the medium TI scan displays zero signal intensity in the midgrey region. This signal may simulate tissue in the sinuses, etc. This is not a problem with STIR sequence. (c) Increased time may be needed for a low resolution phase calibrating scan for the phase corrected version of the IR sequence. We use a 64 × 64 matrix $SE_{544/44}$ scan, which adds approx-

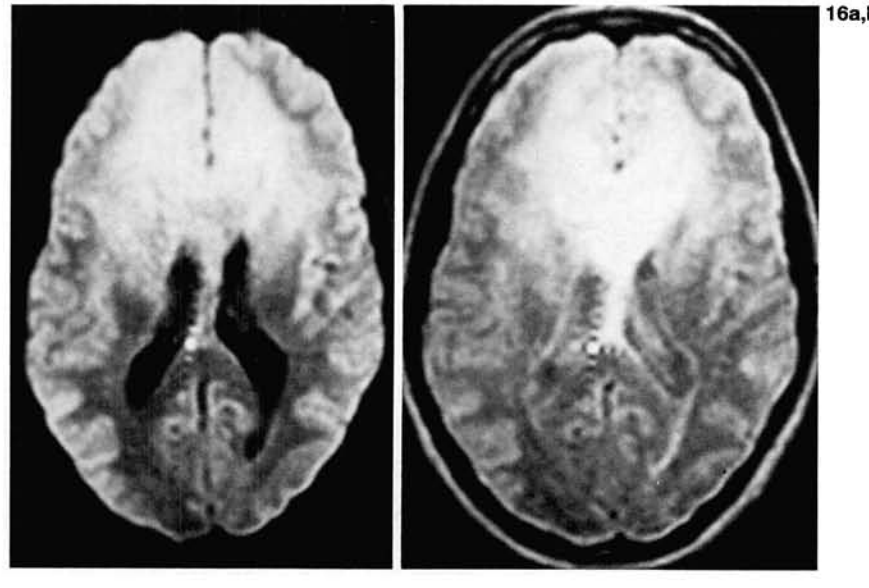

16a,b

FIG. 16. Glioma of the corpus callosum: double inversion recovery $(DIR)_{3,000/1,200/100/44}$ **(a)** and spin echo $(SE)_{1,500/80}$ **(b)** scans. The tumour is well demonstrated on both scans. Both fat and cerebrospinal fluid are suppressed in (a). The ventricular margin is better defined in (a).

17a,b

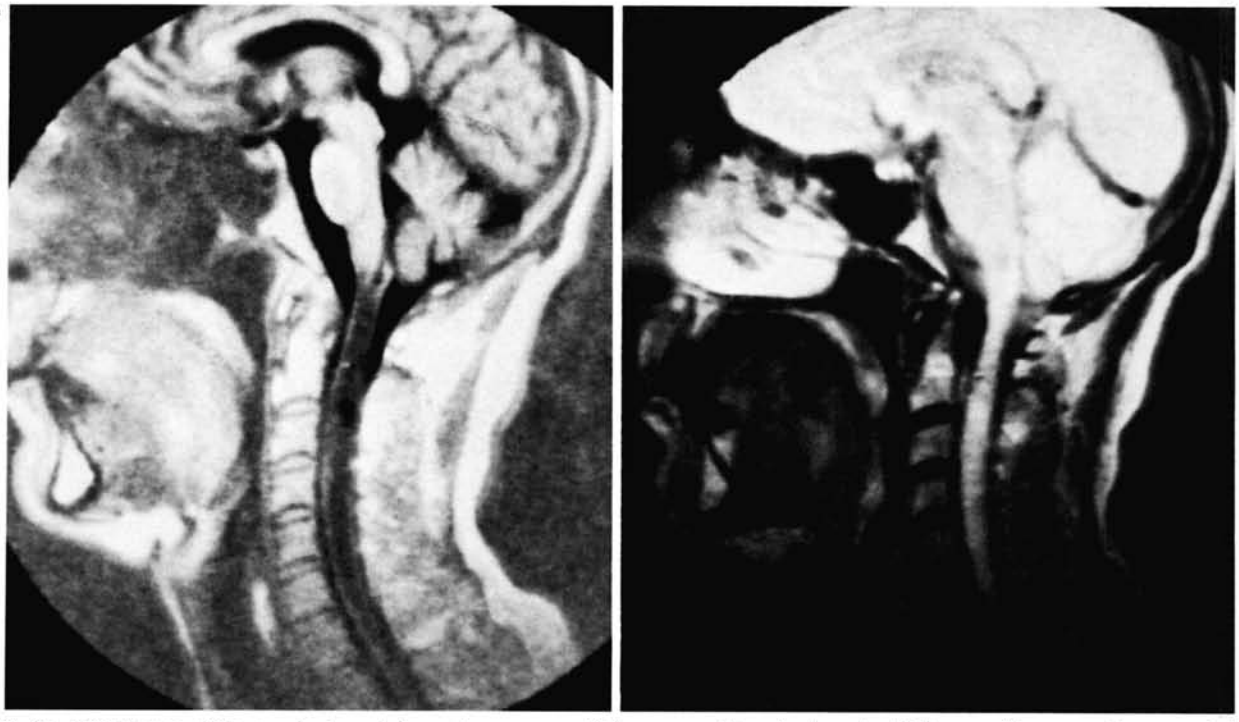

FIG. 17. Lymphoma of the cervical cord: inversion recovery $(IR)_{1,500/500/44}$ **(a)** and spin echo $(SE)_{1,500/80}$ **(b)** scans. Changes within the cord are better seen in (a).

imately 30 s to the imaging time. (d) Radiofrequency pulse calibration needs to be precise for the IR sequence since errors in the angle of rotation of the magnetisation produce a greater loss of tissue contrast than is the case with SE scans (16). This is a greater problem at high field where the loading of the transmitter coil is greater than that at low field. (e) The field echo data acquisition method is more susceptible to magnetic field inhomogeneity than the SE one. Again this problem is greater at high field and limits the value of the short TE field echo data collection.

Advantages of the IR Sequence

As outlined in the introduction the range of possibilities with the IR sequence includes all the options available with both SE and PS scans. It is sensible to use these latter simpler scans in circum-

18a,b

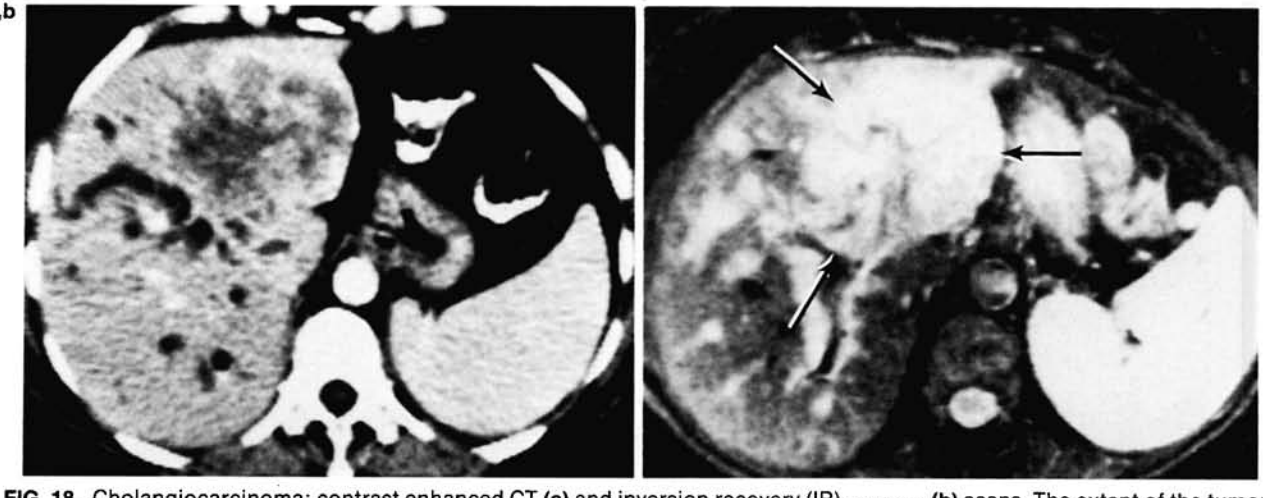

FIG. 18. Cholangiocarcinoma: contrast enhanced CT **(a)** and inversion recovery $(IR)_{1,500/100/44}$ **(b)** scans. The extent of the tumour is well seen in (b) (arrows).

9a,b

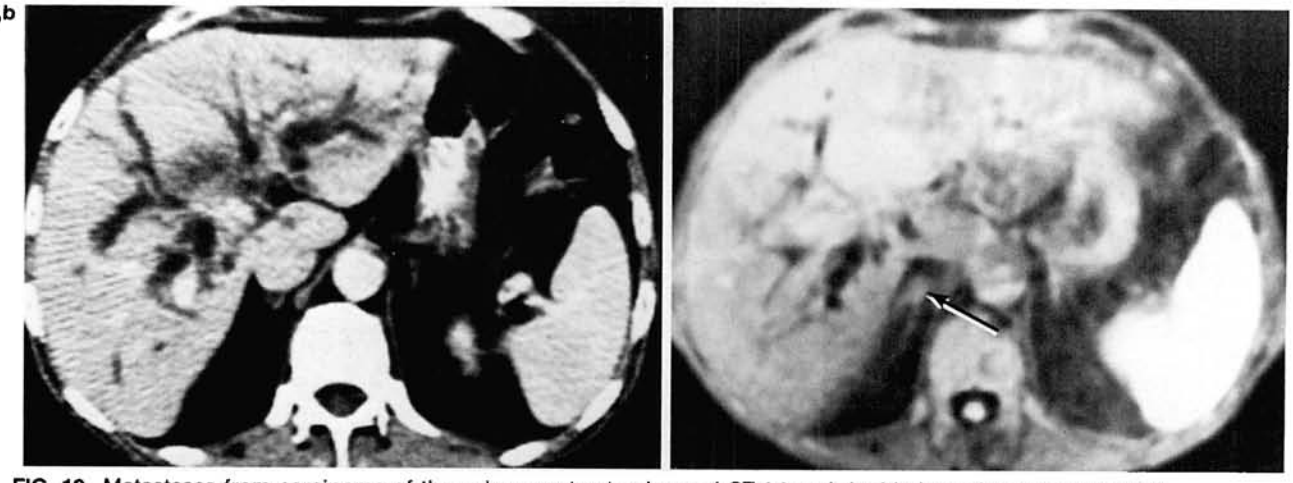

FIG. 19. Metastases from carcinoma of the colon: contrast enhanced CT **(a)** and double inversion recovery $(DIR)_{3,000/1,200/100/44}$ **(b)** scans. Note the adrenal metastasis in (b) (arrow).

stances where there is no particular advantage in using the equivalent more complicated IR scan (e.g., for TI values in the region of 0–30 ms). However, there are many situations in which SE sequences may not provide the best imaging option.

Several particular applications of the IR sequence are worthy of emphasis, as detailed below.

Disease Detection in the Brain

The STIR sequences have a similar sensitivity to the corresponding SE sequences with $IR_{1,500/80/44}$ approximately equivalent to $SE_{1,500/80}$. Although the IR sequences show greater grey-white matter contrast than the SE ones, the signal from CSF can be kept lower than that from brain by reducing TR or TI. Where the lesion is not periventricular and there is no problem with having the CSF signal greater than brain (or a benefit in having it greater), longer values of TE, TR, and TI can be used. The advantage of the DIR sequence is that it allows longer values of these parameters to be used but keeps the CSF signal below that of brain to avoid confusion with partial volume effects in the periventricular region, which is a frequent site of relatively subtle pathology. This may be of particular value at higher fields where it is more difficult to obtain an SE sequence with a high level of lesion contrast and keep the CSF signal less than brain, because the T1 of brain is closer to that of CSF.

Localisation of Lesions and Mass Effects

Although the T2 dependence of most medium TI IR sequences reduces their sensitivity in disease detection, the high level of grey-white matter contrast provides a series of interfaces of value in the localisation of lesions and assessment of mass effects.

20a,b

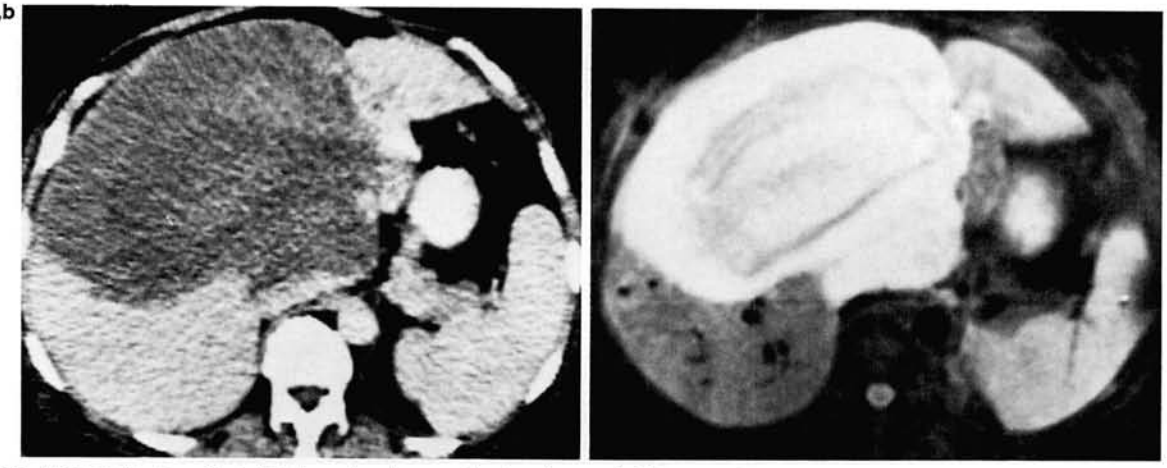

FIG. 20. Hemangioma with left lobe atrophy: contrast enhanced CT **(a)** and inversion recovery $(IR)_{1,500/100/44}$ **(b)** scans. The atrophic left lobe is highlighted in (b).

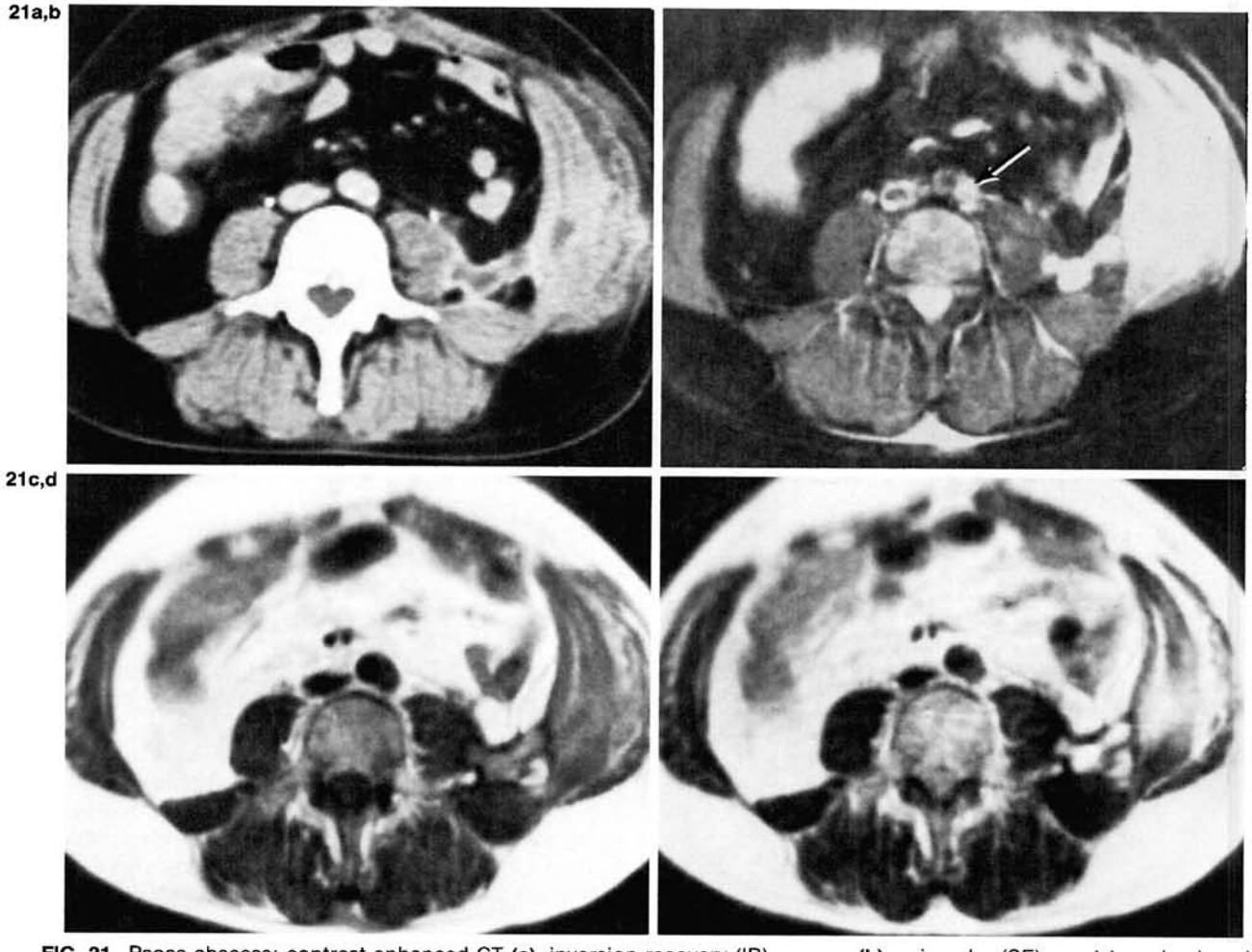

FIG. 21. Psoas abscess: contrast enhanced CT **(a),** inversion recovery $(IR)_{1,000/100/44}$ **(b),** spin echo $(SE)_{544/44}$ **(c),** and spin echo $(SE)_{1,500/80}$ **(d)** scans. Changes to the abdominal wall and the fluid tracking posteriorly are best shown in (b) as is the paraaortic lymph node (arrow).

Pediatrics

The medium or long TI IR sequences provide excellent demonstration of normal myelination as well as delays or deficits in this process. In addition, the fact that the T2 of the neonatal and infant brain is longer than that of adults means that IR sequences are less T2 dependent and therefore of more value in disease detection. The high water content of infantile brain (85–95%) means that oedema is often not so obvious and that oedema detection alone with an SE sequence is a less rewarding strategy in infants than adults. Age adjusted IR sequences are listed in Table 3, although in follow-up studies there is a dilemma in knowing whether to keep the sequence constant or adjust it for age.

Contrast Enhancement

Paramagnetic contrast agents produce the opposite effect to most disease processes; they decrease both T1 and T2. The most sensitive sequence for detecting contrast enhancement is the medium TI IR sequence (with TI intermediate between the lesion T1 before and after contrast enhancement), with the short TE and short TR SE next best, and the long TE and long TR SE least sensitive (6,11,17). This may create a problem when long TE and long TR SE sequences are used for screening purposes since contrast agents (for example, gadolinium-diethylenetriamine pentaacetic acid) may not produce enhancement with this type of sequence. It is therefore necessary to perform an additional preenhancement scan of a different type if a contrast agent is used, so increasing the total time of examination.

Note that, with sequences such as the medium TI IR and the SE with a short TE and short TR, there is usually an increase in signal intensity as the concentration of paramagnetic contrast is increased and this is followed by a decrease as the concentration is increased further (11).

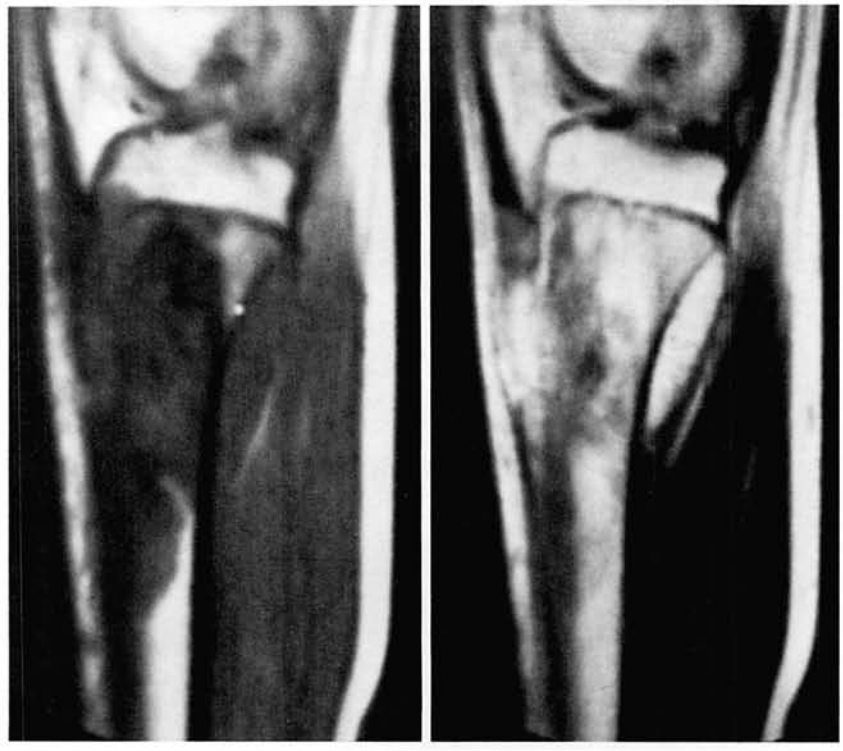

FIG. 22. Osteosarcoma: inversion recovery $(IR)_{1,500/500/44}$ **(a)** and spin echo $(SE)_{1,500/80}$ **(b)** scans. The extent of the tumour is better defined in (a).

Meningiomas and Other "Short T1 Short T2" Tumours

There are a number of tumours including meningiomas that may have a normal or only slightly increased T2 and a normal or low proton density. They usually have a T1 increased over white matter (17–20). With SE sequences there is very little T2 contrast to be exploited, but with medium TI IR sequences the low to normal proton density and slightly increased T1 both tend to reduce signal intensity producing lesion contrast with normal brain and providing better visualisation than with SE sequences (21,22). In addition this group of tumours may show a high level of contrast enhancement and this is best shown with medium TI IR sequences. Since meningiomas have a ubiquitous presentation and are important to exclude, this result has considerable significance in designing a routine screening strategy for MR imaging. The T2 dependence of the medium TI IR sequence, which is usually a significant disadvantage with malignant tumours, is not such a disadvantage with the type of tumour described above, since its T2 is normal or only slightly increased. The same general considerations apply to other tumours of this type (23).

Body Imaging

Although these are "noisy," there are a number of important advantages in using STIR sequences in imaging the body. (a) The T1 and T2 dependent contrast after the 90° is *additive* so that loss of contrast with medium TI IR sequences is not a problem. (b) The STIR sequence provides a high level of tissue contrast using a relatively short TE. This is an advantage because the echo period (TE) in the SE component of the sequence is particularly vulnerable to degradation by motion. (c) The fat signal can be partially or completely suppressed. With long TE long TR SE sequences, the signal intensity of soft tissue lesions is usually increased but this unfortunately brings them into the normal range for fat and thus the margins of the lesion may be lost. This problem can be eliminated by suppressing the fat signal. (d) Much of the respiratory artefact arises from the fat of the anterior abdominal wall producing "ghosts" in the phase encoded direction of the image. Suppression of the fat signal produces a marked reduction in this problem although other techniques are also effective (24,25). We have found the technique of respiratory ordered phase encoding (26) useful in supplementing fat suppression techniques as the signal from spleen or ascites may still act as a source of artefact with STIR sequences. (e) At high fields, chemical shift artefact at the interfaces between fat and water can be a problem. Suppression of the fat signal controls this artefact. (f) Bowel labelling can be achieved with water although the option of using an oral paramagnetic contrast agent is useful to avoid ambiguity with tissues with a long T1 long T2. (g) With surface coils the fat layer adjacent to the coil is normally highlighted as a result of its close prox-

imity, producing difficulties in displaying the image. This is not a problem with fat suppression sequences. (h) In the body, IR sequences can be used to suppress both fluid and fat (DIR sequence) in situations where it is necessary to identify tumour in the presence of dilated bile ducts, to separate urine or cyst from renal tumour, and to control the signal from bowel contents. (i) The difference between the T1 of fat and that of other tissues increases with field, so that the signal intensity from tissues other than fat is relatively higher at higher fields when STIR sequences are used. The images therefore appear less noisy. The T1 of liver is close to that of fat so that it is difficult to obtain a high signal from liver with STIR sequences even at high fields.

The STIR sequence resolves many of the technical problems in MR imaging of the body although the images are noisy. These sequences appear similar to CT scans that have been windowed to show soft tissue except that with MR the level of soft tissue contrast is greater and calcified tissues are not seen. This resemblance corresponds closely to the pattern seen in the brain where MR images resemble CT but show better soft tissue contrast and little calcified tissue.

The theoretical analysis of the IR sequence has received excellent treatment in the literature (7,8,27–30) but little attention has been paid to the clinical application of this sequence, although favourable results have been reported in some specific clinical situations such as intracranial hemorrhage (31,32), brain stem MS (33), and liver disease (34). A notable exception to this general pattern has been the work of the Aberdeen group (35), which has used a medium TI IR sequence with a good quality computed T1 map (the quality of a T1 map computed from IR images is usually better than that computed from two SE sequences of different TR). In many respects the T1 map functions like a STIR sequence giving a low signal intensity for fat and a high signal intensity for lesions with an increased T1. Clinically the Aberdeen group has formed a more favourable impression of body imaging with MR (36,37) than most other groups that have put the emphasis strongly on the nervous system. This may be because the Aberdeen sequence pattern is more suited to body imaging than the equivalent SE approach. The IR sequence has also been used more than usual by Droege et al. (28,29), who have also designed a pattern for screening in the brain using a long TE long TR SE sequence coupled with a short TI IR sequence. This may prove a very worthwhile approach.

Acknowledgment: We are grateful to Dr. H. P. Niendorf of Schering A.G. for supply of Gd-DTPA and advice on its use. We are also grateful to the Medical Research Council and the Department of Health and Social Security for their continued support.

REFERENCES

1. Bailes DR, Young IR, Thomas DJ, Straughan K, Bydder GM, Steiner RE. NMR imaging of the brain using spin-echo sequences. *Clin Radiol* 1982;33:395–414.
2. Bydder GM, Steiner RE, Young IR, et al. Clinical NMR imaging of the brain: 140 cases. *AJR* 1982;139:215–36.
3. Doyle FH, Pennock JM, Banks LM, et al. Nuclear magnetic resonance (NMR) imaging of the liver: initial experience. *AJR* 1982;138:193–200.
4. Young IR, Bailes DR, Burl M, et al. Initial clinical evaluation of a whole body nuclear magnetic resonance (NMR) tomograph. *J Comput Assist Tomogr* 1982;6:1–18.
5. Johnson MA, Pennock JM, Bydder GM, et al. Clinical NMR imaging of the brain in children: normal and neurological disease. *AJNR* 1983;4:1013–26; *AJR* 1983;141:1005–18.
6. Carr DH, Brown J, Bydder GM, et al. Gadolinium-DTPA as a contrast agent in MRI: initial clinical experience in 20 patients. *AJR* 1984;143:215–24.
7. Kurtz D, Dwyer A. Isosignal contours and signal gradients as an aid to choosing MR imaging techniques. *J Comput Assist Tomogr* 1984;8:819–28.
8. Wehrli FW, MacFall JR, Shutts D, Breger R, Herfkens RJ. Mechanisms of contrast in NMR imaging. *J Comput Assist Tomogr* 1984;8:369–80.
9. Bottomley PA, Foster TH, Argsinger RE, Pfeifer LM. A review of normal tissue hydrogen NMR relaxation time and relaxation mechanisms from 1–100 mHz; dependence on tissue type, NMR frequency, temperature, species, exercise and age. *Med Phys* 1984;11:425–48.
10. Young IR, Bailes DR, Bydder GM. Apparent changes of appearance of inversion-recovery images. *Mag Res in Med* 1985;2:81–5.
11. Gadian DG, Payne JA, Bryant DJ, Young IR, Carr DH, Bydder GM. Gadolinium-DTPA as a contrast agent in NMR imaging—theoretical projections and practical observations. *J Comput Assist Tomogr* 1985;9:242–51.
12. Meaney TF. Pulse timing for contrast in clinical imaging. In: *Scientific program and book of abstracts, Society of Magnetic Resonance in Medicine, third annual meeting, August 13–17, 1984, New York, NY.* Berkeley, CA: Society of Magnetic Resonance in Medicine, 1984:522.
13. Axel L. Surface coil magnetic resonance imaging. *J Comput Assist Tomogr* 1984;8:381–4.
14. Bydder GM, Butsen PC, Harman RR, Gilderdale DJ, Young IR. Technical note. Use of spherical receiver coils in magnetic resonance imaging of the brain. *J Comput Assist Tomogr* 1985;9:413–4.
15. Bydder GM, Curati WL, Gadian DG, et al. Use of closely coupled receiver coils in MRI: practical aspects. *J Comput Assist Tomogr* (in press).
16. Young IR. Considerations affecting signal and contrast in NMR imaging. *Br Med Bull* 1984;40:139–47.
17. Bydder GM, Kingsley DPE, Brown J, Niendorf HP, Young IR. Magnetic resonance imaging of meningiomas. *J Comput Assist Tomogr* 1985;9:690–7.
18. Araki T, Inouye T, Suzuki H, et al. Magnetic resonance imaging of brain tumors: measurement of T1. *Radiology* 1984;150:95–8.
19. Gyorffy-Wagner Z, England E, Larsson E-M, et al. T1 and T2 measurements in cerebral tumours and normal brain tissue. Presented at the European Society of Nuclear Magnetic Resonance in Medicine, Geneva, Switzerland, October 5, 1984.
20. Baierl P, Bauer M, Obermuller H. Measurements of relaxation times in intracranial tumours—an approach to tissue discrimination. Presented at the "MR 85" meeting Garmisch Partenkirchen, West Germany, January 24–27, 1985.
21. Li DKB, Robertson WD, Foche JS, et al. MR imaging in CNS tumors. *Radiology* 1984;153(P):85.
22. Zimmerman RD. MRI in intracranial meningiomas. In: *Scientific program and book of abstracts, Society of Magnetic*

Resonance in Medicine, third annual meeting, August 13–17, 1984, New York, NY. Berkeley, CA: Society of Magnetic Resonance in Medicine, 1984:779.

23. McKay IM, Bydder GM, Young IR. Magnetic resonance imaging of central nervous system tumors which do not display evidence of an increased T1 and T2. *J Comput Assist Tomogr* (in press).
24. Ehman RL, McNamara MT, Pollack M, Higgins CB. Respiratory gated MRI: evaluation of technical approaches. In: *Scientific program and book of abstracts, Society of Magnetic Resonance in Medicine, third annual meeting, August 13–17, 1984, New York, NY.* Berkeley, CA: Society of Magnetic Resonance in Medicine, 1984:210–1.
25. Runge VM, Clanton JA, Partain CL, James AE. Respiratory gating in magnetic resonance imaging at 0.5 tesla. *Radiology* 1984;151:521–3.
26. Bailes DR, Gilderdale DJ, Bydder GM, Collins AG, Firmin DN. Respiratory ordered phase encoding (ROPE): a method for reducing respiratory motion artefact in magnetic resonance imaging. *J Comput Assist Tomogr* 1985;9:835–8.
27. Bradley WG, Newton TH, Crooks L. Physical principles of nuclear magnetic resonance. In: TH Newton, DG Potts, eds. *Advanced imaging techniques.* San Anselmo, CA: Clavadel Press, 1983:15–61.
28. Droege RT, Weiner SN, Rzeszotarski MS. A strategy for magnetic resonance imaging of the head; results of a semiempirical model, part I. *Radiology* 1984;153:419–24.
29. Droege RT, Weiner SN, Rzeszotarski MS. A strategy for magnetic resonance imaging of the head: results of a semiempirical model, part II. *Radiology* 1984;153:425–33.
30. Hendrick RE, Nelson TR, Hendee WR. Optimising tissue differentiation in magnetic resonance imaging. *Mag Res Imaging* 1984;2:193–204.
31. Sipponen JT, Sepponen RE, Sivula A. Nuclear magnetic resonance (NMR) imaging of intracerebral hemorrhage in the acute and resolving phases. *J Comput Assist Tomogr* 1983;7:954–9.
32. Sipponen JT, Sepponen RE, Sivula A. Chronic subdural hematoma: demonstration by magnetic resonance. *Radiology* 1984;150:79–85.
33. Runge VM, Price AE, Kirshner HS, et al. Magnetic resonance imaging of multiple sclerosis: a study of pulse technique efficiency. *AJR* 1984;143:1015–26.
34. Borkowski GP, Buonocore E, George CR, Go RT, O'Donovan PB, Meaney TF. Nuclear magnetic resonance (NMR) imaging in the evaluation of the liver: a preliminary experience. *J Comput Assist Tomogr* 1983;7:768–74.
35. Mallard JR. The noes have it! Do they? *Br J Radiol* 1982;54:831–49.
36. Smith FW, Mallard JR, Reid A, Hutchison JMS. Nuclear magnetic resonance imaging of liver disease. *Lancet* 1981;1:963–6.
37. Smith FW, Reid A, Hutchison JMS, Mallard JR. Nuclear magnetic resonance imaging of the pancreas. *Radiology* 1982;142:677–80.